Journal of Nanoscience and Technology 2(3) (2016) 151–154

ISSN: 2455-0191

Contents List available at JACS Directory

Journal of Nanoscience and Technology

journal homepage: www.jacsdirectory.com/jnst

Domain Control of ZnO Nanoparticles using a Coaxial Gas-Flow Ar/O_2 Pulse Plasma

H. Shirahata, S. Iizuka*

Department of Electrical Engineering, Graduate School of Engineering, Tohoku University, Aza Aoba 6-6-05, Aramaki, Aoba-ku, Sendai 980-8579, Japan.

ARTICLE DETAILS

Article history:
Received 31 May 2016
Accepted 15 June 2016
Available online 01 August 2016

Keywords:
Zinc Oxide
Nanoparticle Patterning
Pulse Plasma

ABSTRACT

A limited area, to which ZnO nanoparticles are selectively adhered, is called a domain. Formation of the domain was controlled by using a coaxial gas-flow Ar/O_2 pulse plasma. The mechanism of the domain formation was closely related to initial surface condition of Si substrate. Especially, cleaning process was crucial. Here, a patterning of the domain was employed by using a fine mesh as a template. Linear patterning was also established. The formation processes were estimated by SEM and EDX. The technique developed here will be applied to a selective nanoparticle patterning.

1. Introduction

Zinc oxide (ZnO) is an n-type semiconductor with a wide band gap of 3.37 eV, a large exciton binding energy of 60 meV, and high thermal and mechanical stability [1, 2]. ZnO nanostructures such as nanorods and nanoparticles showed a definite promise for an employment in nanoscale devices, including field emitters, UV lasers [3, 4], field-effect transistors [5-7], dye sensitized solar cells [8-12], and gas sensors [13-15]. In addition, spherical ZnO nanoparticle was expected for an application to quantum dot solar cells [16-18]. Further, ZnO are applied to transparent electrodes [19], light-emitting diodes (LEDs) [20-23], and semiconductor materials [24].

Usually, ZnO nanorods and nanoparticles have been produced by vapor-liquid-solid (VLS) process [25], chemical vapor deposition (CVD) [26], sputtering [27] and laser abrasion method [28]. Our group is focusing on a plasma process for the growth of ZnO nanostructures [29]. This process is superior to the other processes for low temperature deposition and large area deposition. Besides, when the energy of plasma is controlled, ZnO thin films or ZnO nanoparticles can be selectively produced. However, very few studies have dealt with energy-controlled plasma.

In this report, formation of ZnO nanoparticles domain was investigated by focusing on its dependence on the initial surface condition of Si substrate.

2. Experimental Methods

Fig. 1 shows a schematic of the experimental apparatus [30]. The experiment was performed in a low-pressure plasma by employing reactive ion sputtering. As a source of Zn, a zinc rod electrode was used and installed in a glass tube. The flow rates of Ar and O_2 gases were adjusted by mass flow controllers independently and the mixed gas was introduced into a stainless tube with a rod electrode. A negative square-pulse voltage with pulse width of 5 μs was employed for the plasma production.

Partial pressure ratio of Ar/O_2, pulse repetition frequency and supplied voltage were controlled as a parameter. The substrate used was a Si wafer (p-type with crystal orientation of <100>), the surface of which was cleaned by methanol before the experiment. It was possible to change the gas pressure ratio Ar/O_2, input power and substrate position. The wavelength of the optical emission from the plasma was measured by optical emission spectroscope (OES). ZnO deposition was analyzed by scanning electron microscope (SEM) and energy dispersive X-ray spectroscopy (EDX).

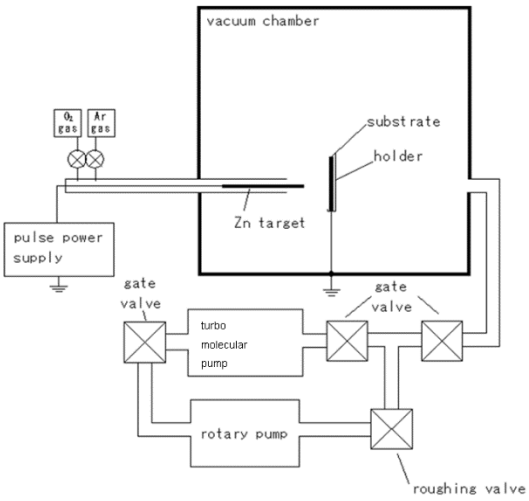

Fig. 1 Schematic representation of experimental setup

3. Results and Discussion

The experiment was conducted when O_2 and Ar flow rates were fixed at 25 and 25 sccm, respectively, i.e., $Ar/O_2 = 1/1$, and the total pressure was 30 Pa. From the results of OES, the emission spectra of Ar and O_2 were observed, but those of Zn were not clearly observed. Therefore, our experimental condition was in an oxide mode. The surface of the Zn electrode was oxidized by O_2 and covered with ZnO thin layer during the deposition experiment.

In our experiment, the sputtering took place only in a short pulse width of 5 μs. The sputtered ZnO molecules from the electrode would react and coagulate each other, and finally grow as clusters and nanoparticles of ZnO during the pulse-off time interval. Fig. 2 shows typical SEM images of the depositions on the Si substrate after 30 minutes deposition. As clearly shown in Fig. 2(a), many nanoparticles were observed only in a limited area forming a domain indicated by an arrow. Almost no nanoparticles were observed outside the domain. The shape of the domain was quite irregular and the domain size was in a range of 20 - 200 μm, much larger

*Corresponding Author
Email Address: iizuka@ecei.tohoku.ac.jp (S. Iizuka)

than the nanoparticles. The size of the domain was enlarged with discharge time, and finally several domains were merged into one big domain. Fig. 2(b) shows a magnified image of nanoparticles deposited in the domain shown in Fig. 2(a). Many nanoparticles of average size of 150 nm are observed. Particle size is quite uniform with an irregularity of 10 %. From EDX analysis and Raman spectroscopy these particles are consisted of ZnO [30].

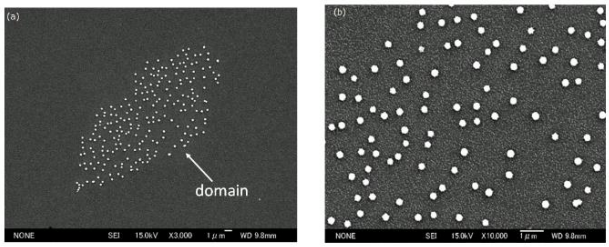

Fig. 2 (a) Formation of a domain, a limited area, to which inside nanoparticles are selectively adhered; Outside the domain no particle is adhered, and (b) Nanoparticle distribution inside the domain. The particle size is quite uniform.

Particle density and particle size were increased with deposition time. A cross-sectional TEM image of the deposition on Si substrate is shown in Fig. 3. One nanoparticle with irregular shape is found to be adhered to the surface of the background layer deposited on the Si surface. It was remarkable that there were no particles buried in the background layer. Therefore, these particles were supposed to grow in a space of plasma. Then, these particles were transported toward the substrate and adhered to the surface of background layer grown on Si substrate, when the discharge was switched off. If the particles were attached to the substrate surface during the discharge, a thin film same as the background layer should cover the particles as well as the background layer. As a result, the particles would be buried in the background layer. The result in Fig. 3 can be explained only when the particles arrive at the surface of background layer after the growth of the background layer. That is, the particles growing in the plasma attached to the background layer surface at the time when the discharge was switched off.

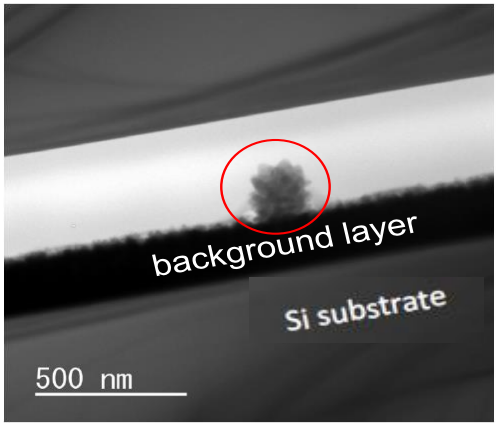

Fig. 3 Cross sectional view of the deposition inside the domain, shown in Fig. 1. One nanoparticle, shown by a red circle, adhered to top surface of background layer deposited on Si substrate.

It is well known that the particles of several 100 nm can be charged negatively by electron attachment in the plasma [31]. These charged nanoparticles would be electrically trapped and levitated at the sheath edge in front of the substrate. Finally, these particles would be detrapped, when the discharge was switched off. Then, these particles were transported toward the substrate and arrived at the surface, and adhered to the surface of the background layer just after switching off the plasma discharge. The particle size and density were increased with time during their trapping.

Next question is why the domain is produced. The nanoparticles levitated in the sheath edge would distribute homogeneously in front of the substrate because of the force balance acting on these particles in the space, i.e., gravity, ion drag, force and electrostatic forces. On the other hand, condition of the surface of the background layer might be inhomogeneous, depending on the initial Si surface condition. Therefore, the particle adhesion was supposed to be caused by such surface condition. Assuming that there existed surface charge inhomogeneity on the background layer, negatively charged nanoparticles would preferably move to relatively positive area by attractive force acting on the particles, rather than to relatively negative area evolving repulsion force. The surface charge inhomogeneity of the background layer would depend on the initial condition of Si substrate.

In order to verify the above hypothesis, two deposition processes were adopted, i.e., the first step for pretreatment process of Si surface during 5 min deposition, and the second step for successive 30-min deposition process similar to the previous experiment as in Fig. 2. Here, pretreatment in the first step was established by covering Si surface by a fine grid of 635 mesh/inch made of stainless steel (wire diameter 20 μm, wire distance of 40 μm) as schematically shown in Fig. 4(a). ZnO thin film was simultaneously deposited not only on the top wire surface, but also on the Si surface through an open space between wires of mesh. Time duration of 5 minutes is too short to generate visible nanoparticles as in usual experiments. Therefore, only thin background layers made of ZnO film was deposited both on wires and Si surface between wires.

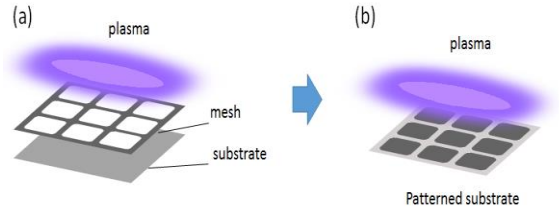

Fig. 4 (a) First step for pretreatment of Si substrate. Patterned Si substrate is produced by plasma sputtering with fine mesh of 635 mesh attached to Si substrate and (b) Second step for main plasma sputtering with a patterned substrate.

After taking out the mesh, the second step deposition was proceeded for 30 min as in Fig. 2, as shown in Fig. 4(b). Fig. 5 shows the depositions on a patterned substrate after the two processes. It was clearly observed that the particles were selectively adhered only to the shallow area (Circle 1) behind the mesh. The close up SEM image is shown in Fig. 6(a), where many nanoparticles are adhered. On the other hand, no nanoparticles were adhered to the open area (Circle 2) between wires of mesh as also shown in Fig. 6(b).

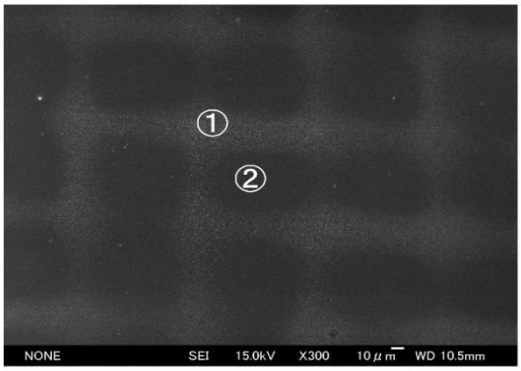

Fig. 5 SEM image of the deposition on patterned Si substrate. Circle 1 corresponds to the shallow area behind wires of mesh. Circle 2 corresponds to the open area between wires of mesh. Nanoparticles are observed only at the area behind wires of mesh (Circle 1).

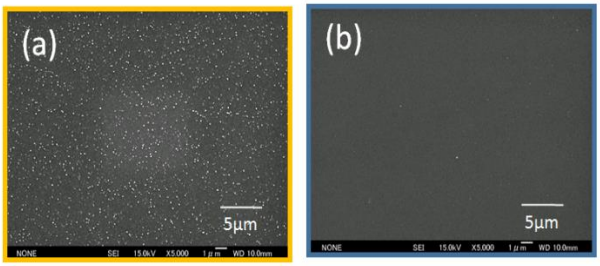

Fig. 6 Magnified SEM images of the depositions on patterned Si substrate (a) behind wires of mesh (Circle 1 in Fig. 5) and (b) between wires of mesh (Circle 2 in Fig. 5). Nanoparticles are observed only in (a), but no particle is adhered in (b).

A model of patterned domain formation in the above processes is schematically shown in Fig. 7. Here, it should be noted that background layer would deposit on the top surface of wires and not deposit on the masked shadow area (Circle 1) of Si surface during the first step, because

the wires of mesh, acting as a mask, made shallow on the Si substrate (see Fig. 7(a)). Here, dotted arrows directed downward show the flow of ions and radicals of ZnO*, Zn*, and O* for the background layer formation. On the other hand, background layer would deposit directly on the open area (Circle 2) of Si surface with the same height as those on the wires, because no shadow effect was acting from wires of mesh. In this way, a patterned substrate with a height difference of background later was produced after the first step treatment. Since the background layer was consisted of ZnO semiconductor, local electric conductivity between the background layer surface and Si surface depends on the height of background layers. Conductivity will be increased in the thin layer (Circle 1), while the conductivity will be relatively low in the thick layer (Circle 2). In the second step, the background layer further grew with an equal height on the patterned substrate as shown in Fig. 7(b). During this growth of background layer, negatively charged nanoparticles were also growing simultaneously in the plasma and levitated in front of the substrate.

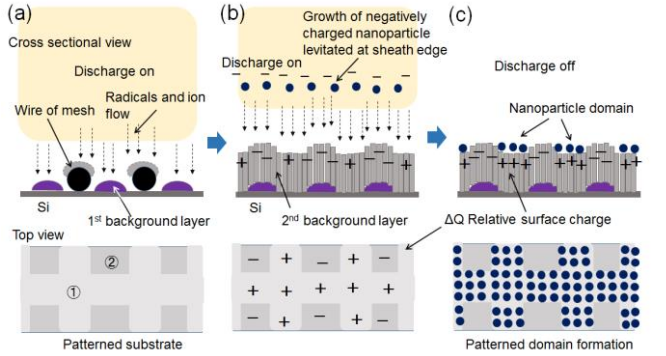

Fig. 7 A model of domain formation. (a) 1st step: patterning of background layer deposition by using wires of mesh as a mask. Dotted arrows directed downward show the flow of ZnO*, Zn*, and O* for background layer formation. Circle 1: masked shadow area, Circle 2: open area with background layer deposited. (b) 2nd step: nanoparticle formation using a patterned substrate. Negatively charged particles are levitated in the plasma. Relative surface charge difference ΔQ induced on background layer surface. And (c) Switching off discharge causes selective adhesion of nanoparticles to patterned less negative charge area to form a patterned domain.

During the discharge, the surface of background layer would be also negatively charged by the electron flow from the plasma, evolving a so-called sheath potential. However, these negative charges would leak to external circuit through background layer and Si substrate with finite conductance. Since such charge leakage depends on the conductivity, there appears patterned inhomogeneity of surface charges ΔQ on the background layer. During the discharge negative surface potential repelled the negatively charged particles. However, once the discharge was switched off, the surface negative charges started to leak to the external circuit through background layer. Decay of negative charges at the thin background layer was faster that that at the thick background layer. Then, relative surface charge difference ΔQ would be induced on background layer surface. Then, the negatively charged nanoparticles could move to such thin film area with relatively positive potential, and could adhere to the background surface as shown in Fig. 7(c). On the other hand, negative charges remained at thick film area would repel negatively charged particles, then no particle adhesion takes place in this area. In this way, the surface charge difference ΔQ evolving on the patterned substrate during the deposition plays a key role for the selective particle adhesion. Negatively charged nanoparticles were preferentially adhered to relatively thin film area patterned by the mesh template and eventually a patterned domain was generated.

As shown in Fig. 2 the domain can be naturally formed without patterning the substrate, although the shape is quite irregular. This domain formation is also related to the initial surface condition of Si substrate. In our experiment the surface of Si substrate was usually cleaned by methyl alcohol. The surface was wiped by hand with fine tissues wetted with methyl alcohol. It was found that initial surface condition was determined by this cleaning process. Here, we adopted the following cleaning process. In the first process, Si substrate surface was wiped by fine tissue with methanol only in one direction linearly for several times, and then, as the second process, the surface was wiped linearly for several times in the other direction with an angle of about 45 decrees with respect to the initial direction. After these cleaning procedures, similar deposition experiment was proceeded under the same conditions as in Fig. 2. The result is shown in Fig. 8, where we can find a linearly aligned nanoparticles along two directions with an angle of about 45 degrees. That is, the nanoparticles are adhered only on lines with different angle made initially in the cleaning process.

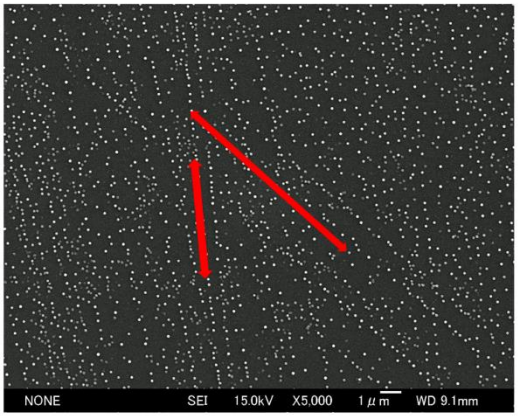

Fig. 8 Linearly aligned nanoparticles arrays in two directions with an angle of about 45 degrees

It was also observed that natural drying process of much amount of methanol after linear wiping caused self-organized circular domains with circular patterns of nanoparticles inside as shown in Fig. 9. Nanoparticles were selectively adhered to circular area, forming a circular domain where nanoparticles arranged circularly inside. The initial patterning would be closely related to an evaporation phenomenon of methanol from Si surface. Methyl alcohol evaporates from Si surface, forming many small circular islands of micron scale during the evaporation, where circularly patterned materials containing methyl bonding might be left on the Si substrate. This technique would be very convenient for an application to a circular domain formation of nanoparticles in future.

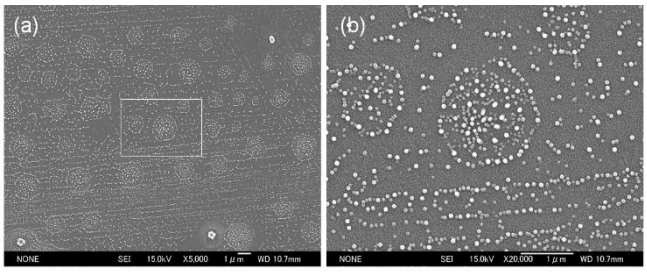

Fig. 9 (a) Self-organized domains of nanoparticles with circular and linear arrangements, and (b) Magnified image of a rectangular area in image (a)

4. Conclusion

We focused on the control of domain formation of ZnO nanoparticles in Ar/O_2 plasmas. The domains could provide only a limited area for the nanoparticles adhesion. The size and shape of the domain produced naturally were quite irregular. However, the shape of the domains was controllable by patterning the substrate surface before the deposition. Our sputtering system was quite effective for controlling nanoparticle adhesion only to a pre-patterned limited and selected area called a domain.

References

[1] C. Jagadish, S.J. Pearton, Zinc oxide bulk, thin films and nanostructures: processing, Properties and applications, Elsevier, Amsterdam, 2006.
[2] Ü. Özgür, Y.I. Alivov, C. Liu, A. Teke, M.A. Reshchikov, et al, A comprehensive review of ZnO materials and devices, J. Appl. Phys. 98 (2005) 041301-1-101.
[3] D.C. Look, B. Claflin, P-type doping and devices based on ZnO, Phys. Status Solidi 241 (2004) 624-630.
[4] S.J. Pearton, D.P. Norton, K. Ip, Y.W. Heo, T. Steiner, Recent progress in processing and properties of ZnO, Prog. Mater. Sci. 50 (2005) 293-340.
[5] N. Bano, S. Zaman, A. Zainelabdin, S. Hussain, I. Hussain, et al, ZnO-organic hybrid white light emitting diodes grown on flexible plastic using low temperature aqueous chemical method, J. Appl. Phys. 108 (2010) 043103-1-5.
[6] W.J.E. Beek, M.M. Wienk, R.A.J. Janssen, hybrid solar cells from regioregular polythiophene and zno nanoparticles, Adv. Funct. Mater. 16 (2006) 1112-1116.
[7] Z.X. Xu, V.A.L. Roy, P. Stallinga, M. Muccini, S. Toffanin, et al, Nanocomposite field effect transistors based on zinc oxide/polymer blends, Appl. Phys. Lett. 90 (2007) 223509-1-3.
[8] K. Keis, E. Magnusson, H. Lindstrom, S.E. Lindquist, A. Hagfeldt, A 5% efficient photoelectrochemical solar cell based on nanostructured ZnO electrodes, Sol. Ener. Mater. Sol. Cells. 73 (2002) 51-58.

[9] J. Yu, Q. Li, Z. Shu, Dye-sensitized solar cells based on double-layered TiO_2 composite films and enhanced photovoltaic performance, Electrochem. Acta 56 (2011) 6293-6298.
[10] P. Raksa, S. Nilphai, A. Gardchareon, S. Choopun, Copper oxide thin film and nanowire as a barrier in ZnO dye-sensitized solar cells, Thin solid films 517 (2009) 4741-4744.
[11] C.C. Yang, H.Q. Zhang, Y.R. Zheng, DSSC with a novel Pt counter electrodes using pulsed electroplating techniques, Curr. Appl. Phys. 11 (2011) S147-S153.
[12] V.M. Guerin, C. Magne, Th. Pauporte, T. Le Bahers, J. Rathousky, Electrodeposited nanoporous versus nanoparticulate ZnO films of similar roughness for dye-sensitized solar cell applications, ACS Appl. Mater. Inter. 2 (2010) 3677-3685.
[13] J.M.S. Spencer, Gas sensing applications of 1D-nanostructures zinc oxide: insights from density functional theory calculations, Prog. Mater. Sci. 57 (2012) 437-486.
[14] S.P. Singh, Sunil K. Arya, P. Pandey, B.D. Malhotra, Cholesterol biosensor based on Rf sputtered zinc oxide nanoporous thin film, Appl. Phys. Lett. 91 (2007) 063901-1-3.
[15] M. Jakobs, S. Muthukukar, A.P. Selvam, J.E. Craven, S. Prasad, Ultra-sensitive electrical immunoassay biosensors using nanotextured zinc oxide thin films on printed circuit board platforms, Biosens. Bioelectron. 55 (2014) 7-13.
[16] J.B. Sambur, T. Novet, B.A. Parkinson, Multiple exciton collection in a sensitized photovoltaic system, Science 330 (2010) 63-66.
[17] C.J. Raj, S.N. Karthick, A.D. Savariraj, K.V. Hemalatha, P. Song-Yi, et al, Electrochemical properties of TiO2 encapsulated ZnO nanorod aggregates dye sensitized solar cells, J. Alloys Compd. 537 (2012) 159-164.
[18] H.M. Cheng, K.Y. Huang, K.M. Lee, P. Yu, S.C. Lin, et al, High-efficiency cascade CdS/CdSe quantum dot-sensitized solar cells based on hierarchical tetrapod-like ZnO nanoparticles, Phys. Chem. 14 (2012) 13539-13548.
[19] R. Jaramillo, S. Ramanathan, Kelvin force microscopy studies of work function of transparent conducting ZnO: Al electrodes synthesized under varying oxygen pressures, Solar energy materials and solar cells, Solar energy materials and solar cells, 95 (2011) 602-605.
[20] S. Calnan, A. Tiwari, High mobility transparent conducting oxides for thin film solar cells, Thin solid films 518 (2010) 1839-1849.
[21] P. Görrn, T. Rabe, T. Riedl, W. Kowalsky, F. Galbrecht, U. Scherf, Low loss contacts for organic semiconductor lasers, Appl. Phys. Lett. 89 (2006) 161113-1-3.
[22] H. Liu, V. Avrutin, N. Izyumskaya, U. Özgür, H. Morkoç, Transparent conducting oxides for electrode applications in light emitting and absorbing devices, Superlatt. Microstruct. 48 (2010) 458-484.
[23] D.C. Kim, W.S. Han, B.H. Kong, H.K. Cho, C.H. Hong, Fabrication of the hybrid ZnO LED structure grown on p-type GaN by metal organic chemical vapor deposition, Physica B: Cond. Mat. 401-402 (2007) 386-390.
[24] H.Y.S. Al-Zahrani, J. Pal, M.A. Migliorato, Non-linear piezoelectricity in wurtzite ZnO semiconductors nano energy, Nano Energy 2 (2013) 1214-1217.
[25] R.T.R. Kumar, E. McGlynn, M. Biswas, R. Saunders, G. Trolliard, et al, Growth of ZnO nanostructures on Au-coated Si: Influence of growth temperature on growth mechanism and morphology, J. Appl. Phys. 104 (2008) 084309-1-11.
[26] T. Terasako, M. Yagi, M. Ishizaki, Y. Senda, H. Matsuura, S. Shirakata, Optical properties of ZnO films grown by atmospheric-pressure chemical vapor deposition using Zn and H_2O as source materials, Thin solid films 516 (2007) 159-164.
[27] H. Ono, S. Iizuka, Growth of ZnO nanowires in hollow-type magnetron O_2/Ar RF plasma, Thin solid films 518 (2009) 1016-1019.
[28] S.V. Prasad, S.D. Walck, J.S. Zabinski, Microstructural evolution in lubricious ZnO films grown by pulsed laser deposition, Thin solid films 360 (2000) 107-117.
[29] K. Kumeta, H. Ono, S. Iizuka, Formation of ZnO nanostructures in energy-controlled hollow-type magnetron RF plasma, Thin solid films 518 (2010) 3522-3525.
[30] H. Shirahata, S. Iizuka, Generation control of ZnO nanoparticles using a coaxial gas-flow pulse plasma Ar/O_2 plasma, J. Nanopart. 2015 (2015) 410468.
[31] G. Uchida, S. Iizuka, N. Sato, Fine-particle clouds controlled in a DC discharge plasma, IEEE Trans. Plasma Sci. 29 (2001) 274-278.

Cite this Article as: H. Shirahata, S. Iizuka, Domain control of ZnO nanoparticles using a coaxial gas-flow Ar/O_2 pulse plasma, J. Nanosci. Tech. 2(3) (2016) 151–154.